

Spin Transitions in Mantle Minerals

James Badro

Institut de Physique du Globe de Paris, Sorbonne Paris Cité, 75005 Paris, France;
email: badro@ipgp.fr

Ecole Polytechnique Fédérale de Lausanne, CH-1015 Lausanne, Switzerland

Annu. Rev. Earth Planet. Sci. 2014. 42:231–48

The *Annual Review of Earth and Planetary Sciences* is online at earth.annualreviews.org

This article's doi:

10.1146/annurev-earth-042711-105304

Copyright © 2014 by Annual Reviews.

All rights reserved

Keywords

lower mantle, spin transitions, high pressure, mineral physics, experimental petrology

Abstract

Mantle minerals at shallow depths contain iron in the high-spin electronic state. The crystal-field splitting energy increases with increasing pressure, which can favor the low-spin state. Hence, pressure-driven transitions from the high-spin to the low-spin state were proposed as early as the 1960s, and minerals in the lower mantle were suggested to contain iron in the low-spin state. Only in the past 10 years did experiments and calculations prove that iron in mantle minerals transforms from high-spin to low-spin at lower-mantle pressures. This transition has important consequences for volume, thermodynamics, and bonding. In a geophysical framework, the transition would affect the dynamics and thermochemical state of the lower mantle, through combined effects on density, elasticity, element partitioning, and transport properties. These observations provide the basis for a new paradigm of the physics and chemistry in Earth's lower(most) mantle.

1. INTRODUCTION

Earth's mantle is the silicate-rich residue of postaccretionary differentiation through core formation. A petrological way to model the composition of the uppermost mantle is to combine, in the right proportions, the two petrologic end-members of the mantle that are observable at the surface: basalts and peridotites. This hypothetical pyroxene- and olivine-rich rock is called pyrolite (Ringwood 1966). In terms of major elements, the pyrolite model is not so different from geochemical and cosmochemical compositional models of the mantle (Allegre et al. 1995, McDonough & Sun 1995, Lyubetskaya & Korenaga 2007), and high-pressure experiments have shown throughout the years that minerals undergo series of mineralogical and petrologic transformations across the mantle from the Moho to the core-mantle boundary (CMB). In the lower mantle, all mineral phases (olivine polymorphs, pyroxenes, garnets) constituting upper-mantle and transition-zone rocks break down to magnesium silicate perovskite (Pv), ferropericlasite (Fp), and calcium silicate perovskite (CaPv). The ubiquitous lower-mantle rock is therefore composed of those three mineral phases, whose iron-free minerals MgO, MgSiO₃, and CaSiO₃ (and their assemblage in an iron-free lower-mantle rock) do not exhibit any physical or chemical peculiarity. In the presence of iron oxide, Fp and Pv readily form solid solutions by Mg-Fe exchange, giving rise to the electronically complex compounds (Mg,Fe)O Fp and (Mg,Fe)SiO₃ Pv, whereas CaPv remains essentially iron free. This article focuses on iron spin transition occurring in minerals, so from here on I consider only the lower mantle's two iron-bearing phases: Pv and Fp.

Of all Earth's major elements, iron has a very special place from the point of view of crystal chemistry. The specificity of iron comes from the fact that it is a transition metal; unlike the other major elements (Mg, Ca, Si, Al, O) of the bulk silicate Earth, it has partially filled 3*d* electronic orbitals that give rise to a series of possible energy configurations that depend on its atomic environment (ligand or crystal field). Notably, iron adopts different valences, namely metallic (Fe⁰), ferrous (Fe²⁺), and ferric (Fe³⁺) iron, and different electronic configurations, such as high-spin and low-spin states. The aim of this article is to discuss the existence and consequences of pressure-driven spin transition—that is, transitions from high-spin iron to low-spin iron—in mantle minerals. Transport properties such as electrical and thermal conductivity, diffusivity, and viscosity can vary significantly with pressure or temperature because of iron content, whereas they remain almost unperturbed in the iron-free end-members. The physical and chemical complexity of lower-mantle mineralogical assemblages is a direct consequence of the presence of iron.

I urge interested readers to also consult the recent article by Lin et al. (2013) in *Reviews of Geophysics* for a thorough and detailed review of spin transitions in mantle minerals.

2. SPIN STATE ENERGETICS

Iron is a 3*d* transition metal, and its ionic electronic structure is (Ar)3*d*⁶ for Fe²⁺ and (Ar)3*d*⁵ for Fe³⁺. The 3*d* orbitals comprise a subset of five orbitals with different symmetry. Three of these (*d*_{xy}, *d*_{xz}, *d*_{yz}) make up a set of atomic orbitals named *t*_{2g}, and the two others (*d*_{x²-y²} and *d*_{z²-y²}) make up a set of atomic orbitals named *e*_g (**Figure 1**). Iron can be in the high-spin (HS) or low-spin (LS) state. These states are defined by the electron occupation of the outermost 3*d* orbital. Their energetic fine structure is shown in **Figure 1** in the case of an octahedral (6-fold coordination) field, within the framework of crystal field theory (Burns 1993).

We can use the framework of crystal field theory to estimate the electronic contributions to internal energy and entropy of an HS or LS state. In case of partially filled orbitals, electrons occupy the orbitals according to a certain number of quantum rules (symmetry, minimization, etc.), and there are two competing energies that need to be minimized: the pairing energy and

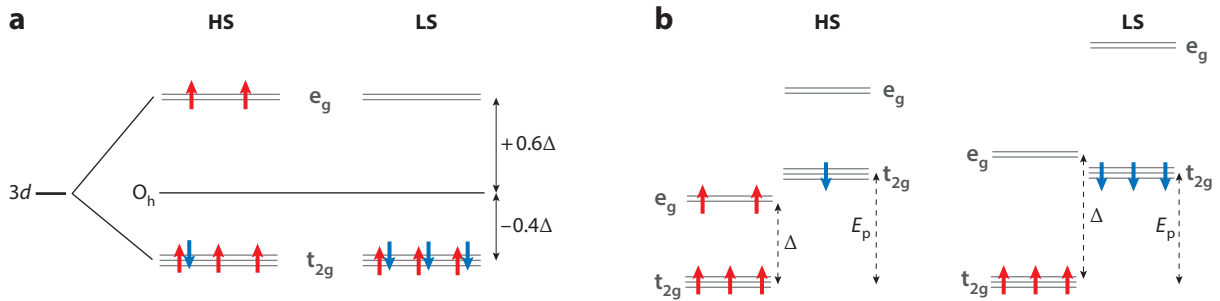


Figure 1

Electronic fine structure of the last unfilled electronic orbital ($3d^6$) of Fe^{2+} in the high-spin (HS) and low-spin (LS) states in an octahedral (O_h) field. (a) The population of both states in terms of orbital symmetry (t_{2g} and e_g). (b) The energetic diagram as a function of the crystal field splitting energy Δ and coulomb repulsion energy E_p . In the case of Fe^{3+} ($3d^5$), which has one less electron, one electron needs to be removed: the spin-down electron in the HS state or any electron (they are all degenerate) in the LS state. HS Fe^{3+} has the highest possible moment, with five spin-up electrons, and LS Fe^{2+} has the lowest possible moment of zero.

the splitting energy between orbitals. Depending on the values of the pairing energy (E_p) and the t_{2g} - e_g splitting energy (Δ , often referred to as the crystal field stabilization parameter), the lowest-energy configuration can be either the HS state (high E_p/Δ ratio, or weak field), where the spin quantum number is maximal, or the LS state (low E_p/Δ ratio, or strong field). The crystal field stabilization parameter Δ increases with decreasing iron-oxygen bond length, and thus with increasing density, whereas the pairing energy remains essentially unchanged; therefore, an iron-bearing mineral with HS iron at low pressure (in the shallow mantle, for instance) can undergo an HS-to-LS transition, or spin pairing transition, at higher pressure (at depth) for the sake of energy minimization.

The internal energy in the HS and LS states of Fe^{2+} is obtained by summing the energies of all six electrons, determined by their energy level and pairing, and one therefore obtains (see **Figure 1**)

$$\text{Fe}^{2+} \begin{cases} U_{\text{HS}} = 4(-0.4\Delta) + 2(0.6\Delta) + E_p = -0.4\Delta + E_p \\ U_{\text{LS}} = 6(-0.4\Delta) + 3E_p = -2.4\Delta + 3E_p \end{cases}$$

$$\text{Fe}^{3+} \begin{cases} U_{\text{HS}} = 3(-0.4\Delta) + 2(0.6\Delta) = 0 \\ U_{\text{LS}} = 5(-0.4\Delta) + 2E_p = -2.0\Delta + 2E_p \end{cases}$$

The electronic configurational entropy is given by $S = k_B \ln(n(2s + 1))$, where s is the total spin, n the orbital degeneracy (at mantle temperature), and k_B the Boltzmann constant (Sherman 1991):

$$\text{Fe}^{2+} \begin{cases} s_{\text{HS}} = 2, n_{\text{HS}} = 3 \Rightarrow S_{\text{HS}} = k_B \ln(15) \\ s_{\text{LS}} = 0, n_{\text{LS}} = 1 \Rightarrow S_{\text{LS}} = 0 \end{cases}$$

$$\text{Fe}^{3+} \begin{cases} s_{\text{HS}} = 2.5, n_{\text{HS}} = 1 \Rightarrow S_{\text{HS}} = k_B \ln(6) \\ s_{\text{LS}} = 0.5, n_{\text{LS}} = 3 \Rightarrow S_{\text{LS}} = k_B \ln(6) \end{cases}$$

Finally, the volume of LS iron is always smaller than that of HS iron. In an octahedral site, an HS Fe^{2+} atom has a radius on the order of 92 pm, which drops to 75 pm in LS Fe^{2+} . The figures for Fe^{3+} are 78.5 and 69 pm for the HS and LS species, respectively.

These three parameters allow us to calculate the Gibbs free energies of the HS and LS species and to apply them to a condensed system (Badro et al. 2005). Indeed, the simple molecular energetic model depicted above can be applied to a condensed system with low iron concentration,

where Fe-Fe interactions and band structure do not play a large role. This is the case for most geologically relevant materials. A more accurate model of the cooperative system can also be treated within mean field theory by applying the Bragg–Williams approximation, as first proposed by Sturhahn et al. (2005), or within density functional theory (DFT) by applying the local density approximation, as first done by Tsuchiya et al. (2006).

What is notable about the spin energetics is that E_p is, to a large extent, independent of pressure or temperature, whereas Δ , which is linked to site geometry and interatomic distances around the iron atom, increases with compression according to (Burns 1993)

$$\Delta(V) = \Delta^0 \left(\frac{V_0}{V} \right)^{5/3},$$

so that for a critical value of Δ , the Gibbs free energy of the LS state becomes lower than that of the HS state, and the system undergoes a spin pairing transition (also known as spin crossover).

3. MEASURING SPIN TRANSITIONS

William Fyfe (1960) proposed over 50 years ago that iron spin pairing takes place in mantle minerals at high pressure, but it was only recently that these transitions were observed experimentally. Spin transitions lead to a number of mineralogical effects (density increase, magnetic reordering, etc.) that can be detected by various techniques. However, spin transitions were first discovered in the mantle minerals Fp (Badro et al. 2003) and Pv (Badro et al. 2004) thanks to synchrotron-based X-ray emission spectroscopy (XES), a spectroscopic technique that allows direct probing of the macroscopically averaged spin of a specific atomic species. To this day, XES remains an essential spectroscopic tool to study spin transitions (Lin et al. 2005, 2007a; Fujino et al. 2012). As these studies have gotten more detailed, XES has been coupled to X-ray diffraction (Lin et al. 2005, Fei et al. 2007, Grocholski et al. 2009, Catalli et al. 2010b), which allows the measurement of small volume changes or discontinuities in the first or second derivatives of the equations of state that are linked to spin transition, or synchrotron Mössbauer spectroscopy (Jackson et al. 2005, Catalli et al. 2010a, McCammon et al. 2010), which allows selective probing of the magnetic states of different valences (Fe^{3+} versus Fe^{2+}).

4. SPIN TRANSITIONS IN LOWER-MANTLE MINERALS

4.1. (Mg,Fe)O Ferropericlas

$(\text{Mg}_{1-x}\text{Fe}_x)\text{O}$ Fp is a simple mineral with the face-centered cubic (fcc) crystallographic structure of MgO, in which Mg atoms have been substituted with Fe atoms. It usually contains one valence of iron (i.e., Fe^{2+}) that is present in the only cation site of the structure, i.e., the standard octahedral site. The initial report of a pressure-induced spin transition in Fp (Badro et al. 2003) occurring between 50 and 70 GPa was made on the basis of an XES study of the spin state and measured the spin magnetic moment of iron in $(\text{Mg}_{0.83}\text{Fe}_{0.17})\text{O}$ Fp, a best proxy for mantle Fp composition.

This initial report was subsequently corroborated by various experimental investigations using XES (Lin et al. 2005), Mössbauer spectroscopy (Speziale et al. 2005), X-ray diffraction (Fei et al. 2007), and impulsive stimulated light scattering (Crowhurst et al. 2008), and by theoretical calculations using thermodynamics (Sturhahn et al. 2005) and DFT (Tsuchiya et al. 2006). This leaves no doubt today that Fp undergoes a spin transition in the 50–70 GPa range at room temperature.

This transition is accompanied by a volume collapse to that of periclase (MgO), resulting in a density increase at lower-mantle pressures (Lin et al. 2005, Speziale et al. 2005, Fei et al. 2007).

An important step forward was to gauge the effect of composition (iron content) and temperature on the spin transition. The effect of composition was studied by XES (Lin et al. 2005) and X-ray diffraction (Speziale et al. 2005, Fei et al. 2007) experiments as well as DFT calculations (Persson et al. 2006), all of which showed that spin crossover pressure increases with increasing iron content, from ~50 GPa for (Fe_{0.2}Mg_{0.8})O to ~70 GPa for (Fe_{0.5}Mg_{0.5})O to ~90 GPa for (Fe_{0.8}Mg_{0.2})O (Speziale et al. 2005), yielding an empirical law for spin transition pressure (in GPa):

$$P_{\text{HS-LS}}^{\text{Fp}}(x_{\text{Fe}}) = 67x_{\text{Fe}} + 37.$$

Another important accomplishment was the ability to directly measure the spin transition at mantle temperatures rather than extrapolate the pressure by using thermal expansion. XES measurements in the laser-heated diamond anvil cell (Lin et al. 2005) allowed that breakthrough and demonstrated that not only do spin transitions occur in mantle minerals at high pressure, but they also occur in the true conditions of the lower mantle, namely high pressure and temperature. In the early days of the spin transition frenzy, many doubted the relevance of spin transitions to the actual mantle and put forth the idea that these transitions were irrelevant at high temperature.

The high-temperature measurements (Lin et al. 2005, Fei et al. 2007) corroborated the thermodynamic prediction (Sturhahn et al. 2005) that these spin transitions were not abrupt transformations occurring in a narrow pressure range, and that they instead occurred over a fairly large pressure range. The initial report of spin transition in Fp (Badro et al. 2003) suggested a ~10–15 GPa pressure range where HS and LS species coexist. The high-temperature experiments showed that this range increases with temperature to 30 GPa (Lin et al. 2005, Sturhahn et al. 2005) at mantle temperature, clearly demonstrating that the effect of these transitions in the mantle would occur over a very large depth range, of approximately 1,000 km. Hence, notably, we do not view spin transitions like narrow mineralogical transitions (such as the α - β , β - γ , and spinel-perovskite transitions in the mantle) that arise sharply at a given depth but rather in the context of a large zone where the properties of iron-bearing minerals change smoothly and gradually. **Figure 2** schematically describes the evolution of the spin state in Fp as a function of pressure, temperature, and composition.

4.2. (Mg,Fe)SiO₃ Perovskite

Spin transitions in Pv were discovered in 2004 (Badro et al. 2004), once again by using XES to probe the spin state and measure the spin magnetic moment of iron, in this case in (Mg_{0.9}Fe_{0.1})SiO₃ Pv. This experiment showed more complex behavior than that observed for Fp, and because Pv is the major phase in the lower mantle, the discovery sparked a general infatuation in the field of mineral physics that led to a remarkable number of studies both experimental and theoretical.

Before reviewing the evidence, it is important to note that one expects not a single transition but a series of transitions in Pv. This is because iron in Pv can be in either the structure's dodecahedral Mg A site or its octahedral Si B site; it can have either valence, Fe²⁺ or Fe³⁺; and it can be in the HS or the LS state (and as discussed below, some investigators have even proposed an intermediate spin state). As a result, there are eight possible (electronic and crystallographic) configurations, incommensurably more intricate than the simple bipolar case (HS and LS) of iron in Fp. This complexity is amplified by the fact that these populations and states should not be considered static; instead, they change with pressure, temperature, and redox state. It has been sensibly proposed

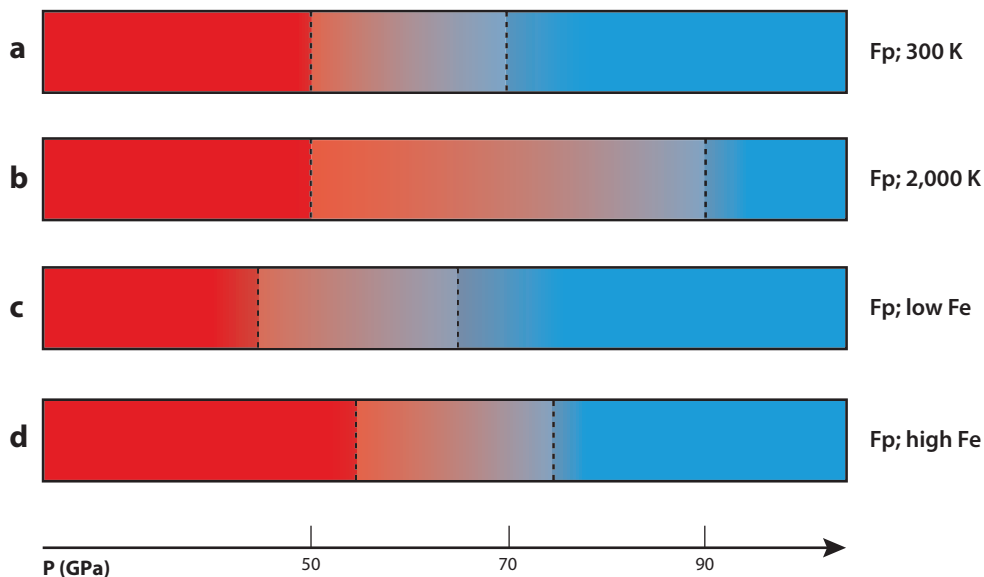


Figure 2

Schematic diagram of spin-state evolution in ferropericlaite (Fp) as a function of pressure, temperature, and composition. Red denotes the high-spin state and blue the low-spin state. (a) The reference state, i.e., room temperature and standard mantle composition: Spin crossover occurs between 50 and 70 GPa. (b) High temperature (2,000 K) and mantle composition: Spin crossover occurs in a larger range, between 50 and 90 GPa. (c) Room temperature and iron-enriched composition: Both onset and final pressures shift upward. (d) Room temperature and iron-depleted composition: Both onset and final pressures shift downward.

that with enough thermal energy to overcome the diffusion barriers, iron migrates between the A and B sites and changes valence and spin state so as to minimize the energy of the system, so that a static description based on macroscopic evidence is unforgivingly obstructed by the microscopic reality of the matter.

In this section, I describe the cumulative discoveries about spin transitions in Pv that have emerged from almost 10 years of research. I separate these discoveries into three chronologically ordered phases.

4.2.1. Phase 1: discovery. In the initial discovery, Badro et al. (2004) reported a gradual transition in the 30–70 GPa range, followed by a sharp transition to a full LS state at 120 GPa. The broad transition was ascribed to iron in the B site and the sharp one to iron in the A site. The samples had been annealed, but postperovskite had not been discovered at that time, so no efforts were made to look for it. That same year another XES study confirmed that the transition to a full LS state was indeed gradual (Li et al. 2004) and was not complete at 100 GPa; more importantly, it showed that the transition depended on the composition of the sample, most importantly the $\text{Fe}^{3+}/\text{Fe}^{2+}$ ratio. The following year, by using synchrotron nuclear forward scattering, which is a redox-selective probe of the magnetic ordering, Jackson et al. (2005) proposed that the gradual changes up to 70 GPa were related to Fe^{3+} undergoing a spin transition. When the first DFT studies were performed (Li et al. 2005), they showed that Fe^{3+} transforms to the LS state over a very large range (60–160 GPa) of lower-mantle pressures (Stackhouse et al. 2007), whereas Fe^{2+} transforms in a much narrower pressure range at 130–145 GPa. This was in surprisingly good

agreement with the experiments (Badro et al. 2004, Jackson et al. 2005) to date and seemed to build on a fairly robust and simple story: Fe^{3+} in the B site (favored by Al incorporation) undergoes a gradual transition from HS to LS between 30 and 70 GPa, and Fe^{2+} in the A site undergoes a sharp transition at 120 GPa.

4.2.2. Phase 2: intermediate spin, or not? Soon enough, DFT calculations began to unravel the microscopic physics of the transitions, and in doing so opened a Pandora's box. The simple duality of our initial understanding of these transitions (site dependence versus valence dependence) was rapidly challenged when it was proposed that Fe^{3+} in the B site was always in the LS state at lower-mantle pressures, whereas Fe^{2+} in the A site transformed to the LS state only in particular atomic arrangements and configurations (Li et al. 2004, Umemoto et al. 2008). By shedding new light on these transformations, we were uncovering the full complexity of these spin pairing transitions, and just when we least expected it came the report of a new spin state in perovskite (McCammon et al. 2008). This report was based on the appearance of an Fe^{2+} species at high pressure with a very unusual value of the Mössbauer quadrupole splitting. With the associated XES observation of an intermediate value of the macroscopically averaged moment (Lin et al. 2008), the intermediate spin state was proposed. One does not expect such a state to be stable (Grocholski et al. 2009, Hsu et al. 2010), especially at high temperatures, unless the distortion of the site is so large that it profoundly changes the electronic energy configuration landscape (Hsu et al. 2011). This intermediate spin state had never been observed before, even in DFT calculations (Li et al. 2004, 2006; Stackhouse et al. 2007). The calculation of Mössbauer parameters using DFT (Bengtson et al. 2008) showed that (a) an intermediate spin, even if it were stable, would not result in a high quadrupole splitting, and (b) the species with high quadrupole splitting observed in Mössbauer experiments is linked to Fe^{2+} in the A site. The last blow to the ill-fated intermediate state came from a series of calculations (Hsu et al. 2010, 2012) and experiments (Grocholski et al. 2009, Lin et al. 2012) that converged to form the picture we have today, as I describe below.

4.2.3. Phase 3: back to the light. During the third phase, which began in 2010 and continues to the present day, some observations have been getting clearer, and refined experimental investigations are being matched by detailed theoretical calculations, allowing an unprecedented level of sophistication in our understanding of the spin state in Pv. The most notable finding in the corpus of recent experimental work (Grocholski et al. 2009; Catalli et al. 2010a,b; Fujino et al. 2012; Lin et al. 2012) and DFT calculations (Hsu et al. 2010, 2012) is the definitive demonstration that the intermediate spin state is not stable and is irrelevant for Pv. This conclusion allows a less ambiguous understanding of the complex processes that occur during the spin transitions in Pv. More specifically, both theoretical (Hsu et al. 2010, 2011) and experimental (Catalli et al. 2010b, Fujino et al. 2012) studies have shown that the intracrystalline partitioning of iron—that is, the partitioning on iron atoms between the A and B sites—depends on the aluminum content of Pv and on the P-T history of the sample. This means that work performed on annealed samples cannot be directly compared with that done on cold samples, because the crystal chemistry is not identical. It also means that in any Al-bearing Pv sample, initial synthesis conditions in multi-anvil presses could dramatically affect the A- and B-site populations, regardless of the subsequent P-T history in the diamond anvil cell.

Experimental investigations on both Al-free (Catalli et al. 2010b) and Al-bearing (Fujino et al. 2012) samples showed that Fe^{3+} enters the A and B sites by charge-coupled substitution (Brodholt 2000) in the case of the Al-free samples and by Fe-Al cation exchange in the case of the Al-bearing samples. The Al-free samples (Catalli et al. 2010b) showed that Fe^{3+} in the B site gradually

transforms from HS to LS with increasing pressure up to 50–60 GPa, at which point all the Fe^{3+} in the B site is in the LS state. Fe^{3+} in the A site remains in the HS state up to at least 136 GPa (CMB pressure). The Al-bearing samples (Fujino et al. 2012) exhibited the same behavior—an LS B site and an HS A site at pressure higher than 50 GPa—but also showed that Al-Fe exchange occurs during annealing (and therefore is expected at mantle temperatures) and that iron migrates from the HS A site to the LS B site, providing an intracrystalline partitioning coefficient that favors the migration of Fe^{3+} to the B site and therefore to the LS state.

Interestingly, DFT calculations (Hsu et al. 2012) are in perfect agreement with the experimental description: Fe^{3+} in the A site is in the LS state at all mantle pressures, whereas Fe^{3+} in the B site goes from HS to LS at high pressure. The presence of aluminum does not affect the spin transitions intrinsically, but it increases the Fe^{3+} concentration in the B site with respect to the A site, through the processes described by Fujino et al. (2012).

The final touch came from the observation of a full LS state for Fe^{2+} in the A site, at 120 GPa (McCammon et al. 2010), in agreement with the first report (Badro et al. 2004). By combining these observations of an LS state for Fe^{2+} at 120 GPa, an LS state for Fe^{3+} in the B site at 70 GPa, and the gradual migration of Fe^{3+} from the HS A site to the LS B site with temperature, it seems possible that iron in perovskite could be in a full LS state in the D' layer ($P > 120$ GPa).

After years of continuous and solid efforts, we are finally starting to get a clearer and more coherent view of the actual processes taking place at the atomic scale during these transitions. Interestingly, these studies show that the mechanisms proposed in the first reports of the spin transition in Pv (Badro et al. 2004) as well as the relative effect of $\text{Fe}^{2+}/\text{Fe}^{3+}$ iron (Jackson et al. 2005) weren't that far off after all, even if they lacked the power of proof provided since (Catalli et al. 2010b, Fujino et al. 2012). **Figure 3** schematically describes the evolution of the spin state in Pv as a function of pressure.

4.3. (Mg,Fe)SiO₃ Postperovskite

The postperovskite (pPv) transition in MgSiO_3 was discovered in 2004 (Murakami et al. 2004), and it was only a matter of time before the mineral physics community's agitation around spin transitions in mantle minerals extended to this phase. Interestingly, the spin state of iron in pPv was first studied theoretically (Stackhouse et al. 2006) using DFT calculations. Even before spin crossover was studied in Pv (Stackhouse et al. 2007), it was shown that Fe^{2+} in pPv was in the HS state at all mantle pressures, a conclusion that has stood the test of time to this day. That was peculiar in the sense that Pv was proposed to have Fe^{2+} in the LS state (Badro et al. 2004, McCammon et al. 2010) at the same pressure (120 GPa), and a transition from Pv to pPv at greater depths would revert Fe^{2+} from LS back to HS.

A year after this first report, experiments challenged this view, and it was proposed that Fe^{2+} is actually in the intermediate spin state (Lin et al. 2008), which had just been suggested for Pv (McCammon et al. 2008). This was later reinterpreted (Mao et al. 2010, 2011) as Fe^{2+} in the intermediate spin state and Fe^{3+} in the LS state. As with the case of Pv, the possibility of an intermediate spin state for Fe^{2+} was refuted by DFT calculations; these show that Fe^{2+} in pPv is in the HS state at all mantle pressures and that the LS and the intermediate state are unstable and energetically unfavorable. As to Fe^{3+} , it is HS in the A site and LS in the B site, just as in the Pv structure, and this is in agreement with the experiments (Mao et al. 2010). Recent experiments finally brought a stronger voice to that model (Fujino et al. 2013), showing that Fe^{3+} in pPv's B site is always in the LS state in the stability field of the phase, whereas Fe^{2+} is in the HS state, and that no Fe^{3+} is found in the A site.

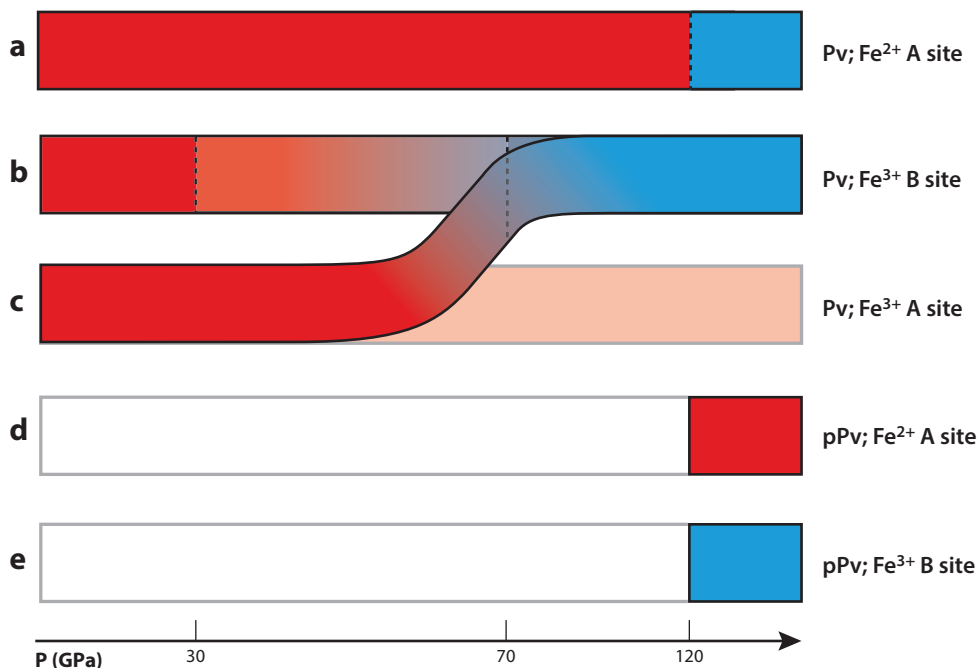


Figure 3

Schematic diagram of spin state evolution in perovskite (Pv) and postperovskite (pPv) as a function of pressure at high temperature. Red denotes the high-spin (HS) state and blue the low-spin (LS) state. (a) Fe^{2+} in the A site goes from HS to LS at 120 GPa. (b) Fe^{3+} in the B site undergoes an HS-LS transition between 30 and 70 GPa. (c) Fe^{3+} in the A-site remains HS at all mantle pressures, but that becomes irrelevant (*shaded area*) as iron atoms migrate toward the B site at 70 GPa, exchanging for aluminum when the B site becomes LS. In the stability range of pPv, (d) Fe^{2+} in the A site remains HS, whereas (e) Fe^{3+} in the B site is always LS.

Keeping in mind that pPv is stable only above 120 GPa in the mantle (Catalli et al. 2009, Grocholski et al. 2012), it is notable that no electronic transitions are found to occur between 120 GPa and the CMB (136 GPa); this implies that pPv is the only lower-mantle phase that always has the same spin state over its entire (albeit limited) stability field. A schematic description of the spin state in pPv is shown in **Figure 3**.

4.4. Silicate Glasses: Proxies for Silicate Melts

The most recent experiments on spin transitions have focused on glasses, used mainly as proxies for deep mantle melts. Surprisingly, the first study (Nomura et al. 2011) on spin crossover in glasses reported a very sharp HS-LS transition (at 75 GPa) in a glass of (iron-bearing) enstatite composition $[(\text{Mg}_{0.8}\text{Fe}_{0.2})\text{SiO}_3]$, much sharper than any observation in crystalline structures (Fp, Pv, pPv). One doesn't expect transitions in glasses to be so sharp, as glass structure changes smoothly and gradually with pressure—much more so than that of crystals—and above all, short-range disorder can promote a large density range of HS and LS coexistence. Subsequent experiments (Gu et al. 2012) on similar systems (augmented with the study of the effect of Al incorporation in the glass) have shown a gradual spin crossover, with the LS component increasing with pressure. Even at the highest pressure of 135 GPa, iron is not fully converted to LS and the samples contain mixtures

of HS and LS iron. These studies are still in their infancy, and the discrepancy will certainly be mitigated as new experimental and theoretical data materialize.

5. GEOPHYSICAL AND GEOCHEMICAL CONSEQUENCES

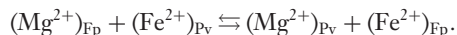
5.1. A Seismic Signature?

One of the first questions to arise is whether spin transitions are geophysically observable. If so, what is their observable signature? Spin transitions are phase transitions, and most phase transitions in mantle minerals are accompanied by density and sound velocity variations that are responsible for the main seismic discontinuities in the upper mantle and transition zone (Agee 1993, Fiquet 2001) and arguably in the D'' region (Murakami et al. 2004). The efforts to gauge the geophysical consequences of spin transitions have naturally focused on finding effects on density or elasticity, because these would directly translate into a global radial seismological signature.

In Fp, initial reports from light scattering (Speziale et al. 2007, Crowhurst et al. 2008) and first principles calculations (Wentzcovitch et al. 2009) proposed a very large softening of the elastic moduli across the spin transition, even though the transition occurs with a small density change (Lin et al. 2005, Fei et al. 2007, Komabayashi et al. 2010, Chen et al. 2012) and no structural change. Seismology would not miss such variations should they occur, but the bulk sound speeds in the lower mantle show no such signs whatsoever (Masters et al. 1996, Cammarano et al. 2010). This apparent discrepancy was recently resolved both theoretically (Caracas et al. 2010) and experimentally (Antonangeli et al. 2011). On the one hand, both studies showed that the spin crossover has no measurable effect on compressional or shear sound velocities, because the change in density is counterbalanced by the change in bulk and shear moduli to a resultant that is null. On the other hand, both studies suggested that there is a strong effect on anisotropy, as already suggested by first principles calculations; in regions with strong anisotropy that develops as a result of texture (lattice-preferred orientation), the spin transition in Fp could have an observable seismological signature.

5.2. Partitioning

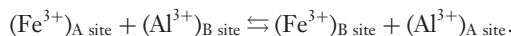
It was proposed very early on that iron spin transitions could have a major influence on its partitioning between minerals (Burns 1993). This effect was highlighted as a main outcome of spin crossover (Badro et al. 2003) and has since been the subject of an ever-growing number of studies. In a typical lower-mantle pyrolytic assemblage, Pv and Fp are in equilibrium, and both Mg and Fe atoms substitute between both minerals according to



The spin crossover of Fe^{2+} in Fp occurs between 50 and 70 GPa at room temperature and between 50 and 90 GPa at mantle temperatures. In Pv, it is unclear whether Fe^{2+} transforms to the LS state, but if it does, this occurs at least at 120 GPa. This means that the major portion of the deep lower mantle (50–120 GPa) comprises an assemblage of LS Fe^{2+} in Fp and HS Fe^{2+} in Pv. In these circumstances, the equilibrium reaction above should be strongly shifted to the right, and iron should preferentially partition into Fp; this is because the LS iron atom occupies a smaller volume than the HS species does, and a preferential partitioning into the LS phase reduces the overall volume of the assemblage, thus minimizing the Gibbs free energy of the system.

Ferric iron cannot substitute for magnesium unless one considers O vacancies in Fp that are highly unfavorable (at low aluminum contents). However, Fe^{3+} partitions internally in the Pv

structure, between the A and B sites, according to



Recent studies have suggested that as Fe^{3+} goes to LS in Pv's B site (at pressures between 50 and 70 GPa), Fe^{3+} in the A site migrates toward this B site, exchanging for Al, exactly following the reaction above.

Numerous experimental studies in the past six years have sought to elucidate iron partitioning in the laser-heated diamond anvil cell, and two opposite trends have been observed. In Fe^{3+} -free systems, where olivine is used as a starting material, Fe^{2+} is indeed enriched in Fp above the spin transition (Auzende et al. 2008, Sakai et al. 2009), between 70 and 120 GPa, and then strongly depleted when pPv appears above 120 GPa. In an pyrolitic (Al- and Fe^{3+} -bearing) composition, the opposite trend has been observed (Sinmyo et al. 2008, Sinmyo & Hirose 2013), with iron enrichment in Pv followed by enrichment in Fp once pPv appears. **Figure 4** illustrates the various trends observed in the literature. The Fe^{3+} -free system is much simpler to understand and model (Badro et al. 2005, Sakai et al. 2009), and it validates the idea that spin crossover drives Fe from the HS to the LS phase. In an Fe^{3+} - and Al-bearing system, crystal chemistry is more complex. Internal partitioning takes place in Pv, as we've seen, between the A and B sites. It has recently been proposed (Sakai et al. 2009, 2010) that the seemingly conflicting observations are in fact due to very different FeO contents in the system and can be unified when using more accurate thermodynamics by taking into account FeO activity in the system. The partition coefficients between silicates and Fp decrease with increasing iron content, which shows that iron has strong activity in Fp. At any rate, these conjectures will probably be substantiated in the years to come by more experimental data and by DFT calculations associated with accurate thermodynamic modeling.

5.3. Viscosity and Diffusivity

Regardless of the direction in which partitioning is affected, strong iron enrichment (2–3-fold) is observed either in Fp or in Pv. Another strong contrast (up to 5-fold) is seen between Fp–Pv and Fp–pPv. Iron enrichment in one phase with respect to the other should have a clear effect on material properties and on the assemblage as a whole. Higher iron concentrations in Mg-rich minerals decrease the melting temperature. At a given temperature along the lower-mantle geotherm, iron-rich minerals should have lower viscosity than their iron-poor counterparts, because the viscosity logarithmically scales with the inverse of melting temperature. A transition that strips one mineral of (most of) its iron, to concentrate it in another, should have a noticeable dynamical signature. It should also have an effect on the buoyancy of the assemblage as a whole; a contrast of up to 1.7% can be calculated from the accurate equations of state (Komabayashi et al. 2010) measured across spin transitions. Add to this a preferential partitioning of iron into Fp, and this density jump could be significantly larger. Of course, Fe^{3+} internal partitioning in Pv is in essence thermodynamically equivalent to Fe^{2+} partitioning between minerals, and the internal redistribution of Fe^{3+} between the sites could have similar effects, but these remain to be evaluated.

Viscosity and chemical transport in the mantle are dependent on diffusion processes, and HS and LS iron do not have the same energetics or local environment and therefore do not have the same migration barriers. DFT calculations have tackled that problem in Fp, on the basis that in the regime where both HS and LS phases coexist, the diffusion of iron through the saddle point could convert LS to HS because of reduced steric effects (Ammann et al. 2011, Saha et al. 2011). The effect was found to be small: The diffusivities change by a factor 1 to 3 across the transition, which should not dramatically affect the rheology of the mantle. However, a strong elastic softening that takes place during spin crossover should also affect viscosity and must also be

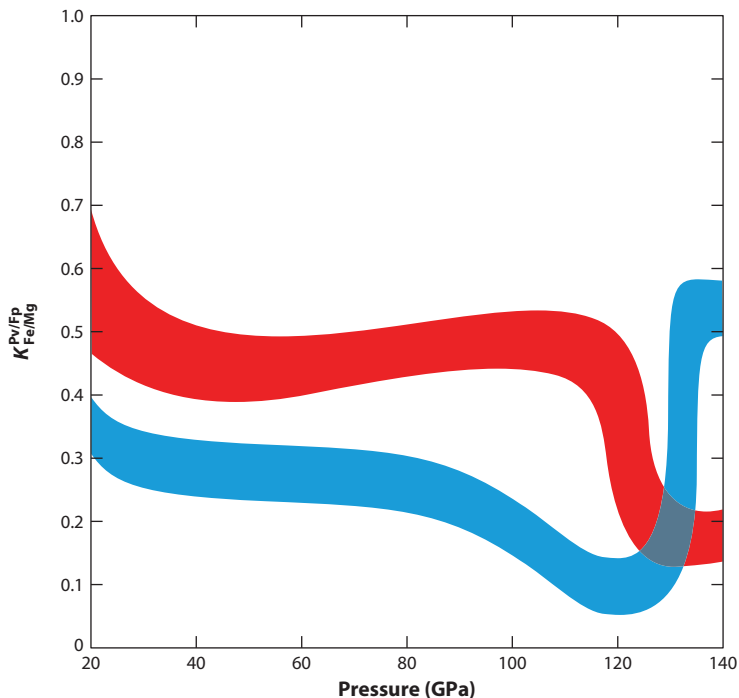


Figure 4

Schematic evolution of the Fe-Mg exchange coefficient (often incorrectly called Fe partitioning) between Pv (or pPv) and Fp. The two trends are rough guides that qualitatively bracket the observations in the literature. The blue trend represents experiments at low Fe^{3+} contents, whereas the red trend represents those at high Fe^{3+} contents. Note that the temperature and composition are not consistent throughout the corpus of data. Refined thermodynamic models can resolve these opposing observations, by correcting for temperature and composition through FeO activity in the system; these models show that under normal conditions, the low- Fe^{3+} model (*blue*) should best describe the partitioning behavior in the mantle. A gradual decrease of iron content in Pv (and iron enrichment in Fp) should occur between 80 and 110 GPa during the spin crossover in Fp, followed by a surge of iron content in silicate above 120 GPa after the transformation to pPv. Abbreviations: Fp, ferropericlae; pPv, postperovskite; Pv, perovskite.

taken into account when estimating rheological properties. DFT calculations have suggested that the viscosity of Fp should drop by 1 to 2 orders of magnitude (Wentzcovitch et al. 2009) because of elastic softening alone. This was further confirmed on the basis of diffusion studies using DFT (Saha et al. 2013), which showed that diffusions associated with spin crossover combined with elastic softening should lead to very large drops in viscosity. In this case the diffusivities of iron drop by a factor of 30, compared with a factor of 3 when softening is not taken into account (Ammann et al. 2011, Saha et al. 2011). This would lead to reductions in viscosity by 1 to 2 orders of magnitude. We must keep in mind, however, that this elastic softening has not been observed in the most recent calculations and experiments, and hence its effect on rheological properties remains to be determined by future studies.

5.4. Thermal and Electrical Conductivity

The first directly measured transport property across the spin transition was electrical conductivity. The number of studies is rather limited, owing to the difficulty of the experiments, but all reports

agree that the electrical conductivity drops across the spin transition in both Fp and Pv. The correlation is rather clear for Fp, for which studies (Lin et al. 2007b, Ohta et al. 2007) have clearly correlated the pressure range of the changes in conductivity (50–70 GPa) with that of spin crossover. In Pv, even though the spin transitions occur over a broad range for ferric iron (30–70 GPa), the conductivity change occurs (Ohta et al. 2010) over a narrow range (70 GPa). One possible explanation is that HS iron is a significantly better conductor, and this could be an indication that as long as it is present, it dominates the conduction process in Pv.

It was proposed early on that spin transitions could affect thermal properties. One of the main and intrinsic characteristics of LS iron-bearing minerals is that their absorption bands are at higher energy (Sherman 1991, Burns 1993) than those of their HS counterparts. Therefore, iron absorption bands shift from the infrared in HS minerals to the visible region in LS minerals, making the latter better thermal conductors. This spawned a renewed interest in the measurement of absorption spectra to estimate the radiative thermal conductivity. Despite some slight disagreements, all the studies show that the spin transition does not dramatically affect radiative thermal conductivity in mantle minerals at the low iron contents of geologically relevant systems.

Infrared absorption measurements were performed on both Fp and Pv at high pressure across the spin crossover. The first study (Goncharov et al. 2006) was performed on Fp containing traces of Fe^{3+} , and no effect was observed across the spin transition. In contrast, the Fe^{3+} -free system (Keppler et al. 2007, Goncharov et al. 2010) revealed a change across the spin transition, with a shift from the infrared to the visible as initially proposed (Badro et al. 2004). The radiative thermal conductivity is expected to increase by only 15% (Keppler et al. 2007), and this should have no geodynamical effect.

Infrared absorption measurements in Pv showed no optical changes related to the transition (Goncharov et al. 2008, Keppler et al. 2008), but the measurements in pPv (Goncharov et al. 2010) showed it had a very high absorbance and was a bad radiative conductor. This phenomenon could have important dynamical effects on the D'' layer, if pPv is the ubiquitous phase in that layer. It could affect the heat flux out of the core, as well as the structure of the thermal boundary layer above the CMB.

5.5. A Note on Transport in a Lower-Mantle Rock

Transport properties of a rock or mineralogical assemblage can be very different from those of a single mineral. It is far from trivial to infer the transport properties of a complex lower-mantle rock on the basis of experiments performed on a single mineral compressed and heated in a diamond anvil cell. The mineralogical view is a good start, but it should not conceal the fact that important data need to be gathered on a high-temperature equilibrium assemblage, where all the effects are taking place concomitantly. Studies of single minerals show little (if any) change in the viscosity, thermal conductivity, or electric conductivity of Fp and Pv across the spin transition, but the fact of the matter is that this could be very different in a rock. If spin pairing causes a strong partitioning behavior between Fp and Pv, as has been observed in several studies, this should also have an effect on transport properties—an effect that cannot be foreseen when studying an isolated mineral. It is not intrinsically linked to the spin transition, but is directly caused by it. This extrinsic effect should dominate the intrinsic effect of the spin pairing transition: Strong iron partitioning in the LS phase (Fp) would make it more opaque and therefore a bad thermal conductor, just as it would render the HS phase (Pv) more transparent and therefore a better thermal conductor. The same applies for viscosity (lower in the iron-rich LS phase and higher in the iron-poor HS phase) and electrical conductivity (higher in the iron-rich LS phase and

lower in the iron-depleted LS phase). A more viscous and more conducting Pv phase, which at ~75–80 vol% dominates the lower mantle, should have strong rheological consequences. However, one realizes that the (highly electrically conductive) Fp phase, at ~20 vol%, is at the threshold of topological interconnectivity. The topology of Pv and Fp in the lower mantle should have dramatic consequences on the dynamical consequences of spin transitions.

6. CONCLUSION

The discovery of spin transitions just over 10 years ago has generated both intense activity in the mineral physics community and broad interest from the geophysical community at large. The picture that emerges is that spin transitions affect all iron-bearing lower-mantle phases: ferroperricite, perovskite, and postperovskite. They cause changes in density, elasticity, chemical diffusivity, and electrical conductivity. They contribute to strong partitioning of iron between the minerals, as well as within (the various sites of) a mineral, and this should strongly affect viscosity and heat conductivity. They are broad and smooth transitions that cover the entire pressure range of the lower mantle. There are still advances to be made, especially by shifting gears from the study of minerals to the study of actual rocks and assemblages. Nevertheless, the mineral physics community has done a terrific job highlighting and quantifying the effects of spin transitions; these efforts leave no doubt that the lower mantle has a smooth complexity just as the upper mantle has a series of sharp features. It is now time for the geophysics and geochemistry communities to incorporate new physics and chemistry in their research, from seismic modeling of lower-mantle anisotropy and D'' structure; to 3D global geodynamical modeling; to core-mantle coupling, heat transfer through the lower mantle, and global chemical geodynamics.

SUMMARY POINTS

1. Spin transitions in iron from the HS to the LS state occur in all lower-mantle minerals at lower-mantle P-T conditions. They are gradual transformations and occur over a broad pressure range.
2. In Fp (17 mol% FeO), we see one HS-LS transition between 50 and 70 GPa at room temperature and between 50 and 90 GPa at mantle temperatures. Higher iron content shifts the transition to higher pressures and lower iron content to lower pressures.
3. In Pv (10 mol% FeSiO₃), a series of transitions are observed. Fe³⁺ in the B site undergoes an HS-LS transition between 30 and 70 GPa. Fe³⁺ in the A site (HS) then migrates to the B site and becomes LS. Fe²⁺ remains in the A site and transforms from HS to LS at 120 GPa.
4. In pPv, Fe³⁺ is in the LS state and Fe²⁺ in the HS state.
5. Iron strongly favors the LS environment, which drives iron partitioning between minerals (Fe²⁺ is depleted in Pv and enriched in Fp), as well as within a mineral (Fe³⁺ in Pv migrates from the HS A site to the LS B site).

DISCLOSURE STATEMENT

The author is not aware of any affiliations, memberships, funding, or financial holdings that might be perceived as affecting the objectivity of this review.

ACKNOWLEDGMENTS

I express my gratitude to Barbara Romanowicz at the University of California, Berkeley, for providing the quiet, still, and tranquil environment for a short sabbatical leave during which I undertook the writing of this manuscript. I am grateful to Joel Dyon, IGP's creative draftsman, for producing most of the figures in this article. I wish to acknowledge financial support from the European Research Council (DECORE, ERC grant agreement number 207467), the French Academy of Science (Grand-Prix Bourcart-Gentil), and the UnivEarthS Labex program at Sorbonne Paris Cité (ANR-10-LABX-0023 and ANR-11-IDEX-0005-02). I thank my son William for keeping me up late at night, and my wife Lydie for waking me up early in the mornings: Their combined efforts extended my days and working hours, albeit at the expense of sharper eyes. I am indebted to the superlative Lavazza Espresso Point professional series espresso pods: a cup "just like in Italy" under the California sun, which helped alleviate the effects of sleep deprivation. Finally, I thank the Annual Reviews editorial team for comments and edits that substantially improved the manuscript.

LITERATURE CITED

- Agee CB. 1993. Petrology of the mantle transition zone. *Annu. Rev. Earth Planet. Sci.* 21:19–41
- Allegre CJ, Poirier JP, Humler E, Hofmann AW. 1995. The chemical composition of the Earth. *Earth Planet. Sci. Lett.* 134:515–26
- Ammann MW, Brodholt JP, Dobson DP. 2011. Ferrous iron diffusion in ferro-periclase across the spin transition. *Earth Planet. Sci. Lett.* 302:393–402**
- Antonangeli D, Siebert J, Aracne CM, Farber DL, Bosak A, et al. 2011. Spin crossover in ferropericlase at high pressure: a seismologically transparent transition? *Science* 331:64–67
- Auzende AL, Badro J, Ryerson FJ, Weber PK, Fallon SJ, et al. 2008. Element partitioning between magnesium silicate perovskite and ferropericlase: new insights into bulk lower-mantle geochemistry. *Earth Planet. Sci. Lett.* 269:164–74**
- Badro J, Fiquet G, Guyot F. 2005. Thermochemical state of the lower mantle: new insights from mineral physics. In *Earth's Deep Mantle: Structure, Composition, and Evolution*, ed. RD Van Der Hilst, JD Bass, J Matas, J Trampert, pp. 241–60. Geophys. Monogr. Ser. 160. Washington, DC: AGU
- Badro J, Fiquet G, Guyot F, Rueff JP, Struzhkin VV, et al. 2003. Iron partitioning in Earth's mantle: toward a deep lower mantle discontinuity. *Science* 300:789–91**
- Badro J, Rueff JP, Vanko G, Monaco G, Fiquet G, Guyot F. 2004. Electronic transitions in perovskite: possible nonconvecting layers in the lower mantle. *Science* 305:383–86**
- Bengtson A, Persson K, Morgan D. 2008. Ab initio study of the composition dependence of the pressure-induced spin crossover in perovskite ($\text{Mg}_{1-x}\text{Fe}_x$) SiO_3 . *Earth Planet. Sci. Lett.* 265:535–45
- Brodholt JP. 2000. Pressure-induced changes in the compression mechanism of aluminous perovskite in the Earth's mantle. *Nature* 407:620–22
- Burns RG. 1993. *Mineralogical Application of Crystal Field Theory*. Cambridge, UK: Cambridge Univ. Press
- Cammarano F, Marquardt H, Speziale S, Tackley PJ. 2010. Role of iron-spin transition in ferropericlase on seismic interpretation: a broad thermochemical transition in the mid mantle? *Geophys. Res. Lett.* 37:L03308
- Caracas R, Mainprice D, Thomas C. 2010. Is the spin transition in Fe^{2+} -bearing perovskite visible in seismology? *Geophys. Res. Lett.* 37:L13309
- Catalli K, Shim SH, Prakapenka V. 2009. Thickness and Clapeyron slope of the post-perovskite boundary. *Nature* 462:782–85
- Catalli K, Shim SH, Prakapenka VB, Zhao J, Sturhahn W. 2010a. X-ray diffraction and Mössbauer spectroscopy of Fe^{3+} -bearing Mg-silicate post-perovskite at 128–138 GPa. *Am. Mineral.* 95:418–21
- Catalli K, Shim SH, Prakapenka VB, Zhao JY, Sturhahn W, et al. 2010b. Spin state of ferric iron in MgSiO_3 perovskite and its effect on elastic properties. *Earth Planet. Sci. Lett.* 289:68–75
- Chen B, Jackson JM, Sturhahn W, Zhang DZ, Zhao JY, et al. 2012. Spin crossover equation of state and sound velocities of ($\text{Mg}_{0.65}\text{Fe}_{0.35}$)O ferropericlase to 140 GPa. *J. Geophys. Res.* 117:B08208

The first study of diffusivity and viscosity across a spin transition.

The first study of iron partitioning between perovskite and ferropericlase across the spin transition.

The first experimental observation of a spin transition in a mantle mineral, namely ferropericlase, occurring at lower-mantle pressures.

The first experimental observation of spin transitions in perovskite.

The first publication suggesting the possibility of spin transition driven by high pressure in mantle minerals.

The first study of absorption and radiative thermal conductivity across a spin transition.

The first DFT calculation of spin transition in perovskite.

- Crowhurst JC, Brown JM, Goncharov AF, Jacobsen SD. 2008. Elasticity of (Mg,Fe)O through the spin transition of iron in the lower mantle. *Science* 319:451–53
- Fei YW, Zhang L, Corgne A, Watson H, Ricolleau A, et al. 2007. Spin transition and equations of state of (Mg,Fe)O solid solutions. *Geophys. Res. Lett.* 34:L17307
- Fiquet G. 2001. Mineral phases of the Earth's mantle. *Z. Kristallogr.* 216:248–71
- Fujino K, Nishio-Hamane D, Kuwayama Y, Sata N, Murakami S, et al. 2013. Spin transition and substitution of Fe³⁺ in Al-bearing post-Mg-perovskite. *Phys. Earth Planet. Inter.* 217:31–35
- Fujino K, Nishio-Hamane D, Seto Y, Sata N, Nagai T, et al. 2012. Spin transition of ferric iron in Al-bearing Mg-perovskite up to 200 GPa and its implication for the lower mantle. *Earth Planet. Sci. Lett.* 317:407–12
- Fyfe WS. 1960. The possibility of *d*-electron coupling in olivine at high pressures. *Geochim. Cosmochim. Acta* 19:141–43
- Goncharov AF, Haugen BD, Struzhkin VV, Beck P, Jacobsen SD. 2008. Radiative conductivity in the Earth's lower mantle. *Nature* 456:231–34
- Goncharov AF, Struzhkin VV, Jacobsen SD. 2006. Reduced radiative conductivity of low-spin (Mg,Fe)O in the lower mantle. *Science* 312:1205–8**
- Goncharov AF, Struzhkin VV, Montoya JA, Kharlamova S, Kundargi R, et al. 2010. Effect of composition, structure, and spin state on the thermal conductivity of the Earth's lower mantle. *Phys. Earth Planet. Inter.* 180:148–53
- Grocholski B, Catalli K, Shim SH, Prakapenka V. 2012. Mineralogical effects on the detectability of the postperovskite boundary. *Proc. Natl. Acad. Sci. USA* 109:2275–79
- Grocholski B, Shim SH, Sturhahn W, Zhao J, Xiao Y, Chow PC. 2009. Spin and valence states of iron in (Mg_{0.8}Fe_{0.2})SiO₃ perovskite. *Geophys. Res. Lett.* 36:L24303
- Gu C, Catalli K, Grocholski B, Gao LL, Alp E, et al. 2012. Electronic structure of iron in magnesium silicate glasses at high pressure. *Geophys. Res. Lett.* 39:L24304
- Hsu H, Blaha P, Cococcioni M, Wentzcovitch RM. 2011. Spin-state crossover and hyperfine interactions of ferric iron in MgSiO₃ perovskite. *Phys. Rev. Lett.* 106:118501
- Hsu H, Umemoto K, Blaha P, Wentzcovitch RM. 2010. Spin states and hyperfine interactions of iron in (Mg,Fe)SiO₃ perovskite under pressure. *Earth Planet. Sci. Lett.* 294:19–26
- Hsu H, Yu YGG, Wentzcovitch RM. 2012. Spin crossover of iron in aluminous MgSiO₃ perovskite and post-perovskite. *Earth Planet. Sci. Lett.* 359:34–39
- Jackson JM, Sturhahn W, Shen GY, Zhao JY, Hu MY, et al. 2005. A synchrotron Mössbauer spectroscopy study of (Mg,Fe)SiO₃ perovskite up to 120 GPa. *Am. Mineral.* 90:199–205
- Keppeler H, Dubrovinsky LS, Narygina O, Kantor I. 2008. Optical absorption and radiative thermal conductivity of silicate perovskite to 125 Gigapascals. *Science* 322:1529–32
- Keppeler H, Kantor I, Dubrovinsky LS. 2007. Optical absorption spectra of ferropericlaite to 84 GPa. *Am. Mineral.* 92:433–36
- Komabayashi T, Hirose K, Nagaya Y, Sugimura E, Ohishi Y. 2010. High-temperature compression of ferropericlaite and the effect of temperature on iron spin transition. *Earth Planet. Sci. Lett.* 297:691–99
- Li J, Struzhkin VV, Mao HK, Shu JF, Hemley RJ, et al. 2004. Electronic spin state of iron in lower mantle perovskite. *Proc. Natl. Acad. Sci. USA* 101:14027–30
- Li J, Sturhahn W, Jackson JM, Struzhkin VV, Lin JF, et al. 2006. Pressure effect on the electronic structure of iron in (Mg,Fe)(Si,Al)O₃ perovskite: a combined synchrotron Mössbauer and X-ray emission spectroscopy study up to 100 GPa. *Phys. Chem. Miner.* 33:575–85
- Li L, Brodholt JP, Stackhouse S, Weidner DJ, Alfredsson M, Price GD. 2005. Electronic spin state of ferric iron in Al-bearing perovskite in the lower mantle. *Geophys. Res. Lett.* 32:L17307**
- Lin JF, Alp EE, Mao Z, Inoue T, McCammon C, et al. 2012. Electronic spin states of ferric and ferrous iron in the lower-mantle silicate perovskite. *Am. Mineral.* 97:592–97

- Lin JF, Speziale S, Mao Z, Marquardt H. 2013. Effects of the electronic spin transitions of iron in lower mantle minerals: implications for deep mantle geophysics and geochemistry. *Rev. Geophys.* 51:244–75
- Lin JF, Struzhkin VV, Jacobsen SD, Hu MY, Chow P, et al. 2005. Spin transition of iron in magnetite in the Earth's lower mantle. *Nature* 436:377–80
- Lin JF, Vanko G, Jacobsen SD, Iota V, Struzhkin VV, et al. 2007a. Spin transition zone in Earth's lower mantle. *Science* 317:1740–43
- Lin JF, Watson H, Vanko G, Alp EE, Prakapenka VB, et al. 2008. Intermediate-spin ferrous iron in lowermost mantle post-perovskite and perovskite. *Nat. Geosci.* 1:688–91
- Lin JF, Weir ST, Jackson DD, Evans WJ, Vohra YK, et al. 2007b. Electrical conductivity of the lower-mantle ferropericlase across the electronic spin transition. *Geophys. Res. Lett.* 34:L16305
- Lyubetskaya T, Korenaga J. 2007. Chemical composition of Earth's primitive mantle and its variance. 1. Method and results. *J. Geophys. Res.* 112:B03211
- Mao Z, Lin JF, Jacobs C, Watson HC, Xiao Y, et al. 2010. Electronic spin and valence states of Fe in CaIrO₃-type silicate post-perovskite in the Earth's lowermost mantle. *Geophys. Res. Lett.* 37:L22304
- Mao Z, Lin JF, Scott HP, Watson HC, Prakapenka VB, et al. 2011. Iron-rich perovskite in the Earth's lower mantle. *Earth Planet. Sci. Lett.* 309:179–84
- Masters G, Johnson S, Laske G, Bolton H. 1996. A shear-velocity model of the mantle. *Philos. Trans. R. Soc. A* 354:1385–410
- McCammon C, Dubrovinsky L, Narygina O, Kantor I, Wu X, et al. 2010. Low-spin Fe²⁺ in silicate perovskite and a possible layer at the base of the lower mantle. *Phys. Earth Planet. Inter.* 180:215–21
- McCammon C, Kantor I, Narygina O, Rouquette J, Ponkratzen U, et al. 2008. Stable intermediate-spin ferrous iron in lower-mantle perovskite. *Nat. Geosci.* 1:684–87
- McDonough WF, Sun SS. 1995. The composition of the Earth. *Chem. Geol.* 120:223–53
- Murakami M, Hirose K, Kawamura K, Sata N, Ohishi Y. 2004. Post-perovskite phase transition in MgSiO₃. *Science* 304:855–58
- Nomura R, Ozawa H, Tatenos S, Hirose K, Hernlund J, et al. 2011. Spin crossover and iron-rich silicate melt in the Earth's deep mantle. *Nature* 473:199–202
- Ohta K, Hirose K, Onoda S, Shimizu K. 2007. The effect of iron spin transition on electrical conductivity of (Mg,Fe)O magnetite. *Proc. Jpn. Acad. B* 83:97–100
- Ohta K, Hirose K, Shimizu K, Sata N, Ohishi Y. 2010. The electrical resistance measurements of (Mg,Fe)SiO₃ perovskite at high pressures and implications for electronic spin transition of iron. *Phys. Earth Planet. Inter.* 180:154–58
- Persson K, Bengtson A, Ceder G, Morgan D. 2006. Ab initio study of the composition dependence of the pressure-induced spin transition in the (Mg_{1-x},Fe_x)O system. *Geophys. Res. Lett.* 33:L16306
- Ringwood AE. 1966. Chemical evolution of the terrestrial planets. *Geochim. Cosmochim. Acta* 30:41–104
- Saha S, Bengtson A, Crispin KL, Van Orman JA, Morgan D. 2011. Effects of spin transition on diffusion of Fe²⁺ in ferropericlase in Earth's lower mantle. *Phys. Rev. B* 84:184102
- Saha S, Bengtson A, Morgan D. 2013. Effect of anomalous compressibility on Fe diffusion in ferropericlase throughout the spin crossover in the lower mantle. *Earth Planet. Sci. Lett.* 362:1–5
- Sakai T, Ohtani E, Terasaki H, Miyahara M, Nishijima M, et al. 2010. Fe-Mg partitioning between post-perovskite and ferropericlase in the lowermost mantle. *Phys. Chem. Miner.* 37:487–96
- Sakai T, Ohtani E, Terasaki H, Sawada N, Kobayashi Y, et al. 2009. Fe-Mg partitioning between perovskite and ferropericlase in the lower mantle. *Am. Mineral.* 94:921–25
- Sherman DM. 1991. The high-pressure electronic structure of magnetite (Mg,Fe)O: applications to the physics and chemistry of the lower mantle. *J. Geophys. Res.* 96(B9):14299–312
- Sinmyo R, Hirose K. 2013. Iron partitioning in pyrolytic lower mantle. *Phys. Chem. Miner.* 40:107–13
- Sinmyo R, Hirose K, Nishio-Hamane D, Seto Y, Fujino K, et al. 2008. Partitioning of iron between perovskite/postperovskite and ferropericlase in the lower mantle. *J. Geophys. Res.* 113:B11204
- Speziale S, Lee VE, Clark SM, Lin JF, Pasternak MP, Jeanloz R. 2007. Effects of Fe spin transition on the elasticity of (Mg,Fe)O magnetites and implications for the seismological properties of the Earth's lower mantle. *J. Geophys. Res.* 112:B10212

A recent and thorough review article on the effect of spin transitions in Earth's lower mantle.

The first experimental observation of a spin transition at combined high pressure and temperature, at lower-mantle P and T.

The first study of electrical conductivity across a spin transition.

The first DFT
calculation of spin
transition in
ferropericlaase.

- Speziale S, Milner A, Lee VE, Clark SM, Pasternak MP, Jeanloz R. 2005. Iron spin transition in Earth's mantle. *Proc. Natl. Acad. Sci. USA* 102:17918–22
- Stackhouse S, Brodholt JP, Dobson DP, Price GD. 2006. Electronic spin transitions and the seismic properties of ferrous iron-bearing MgSiO₃ post-perovskite. *Geophys. Res. Lett.* 33:L12S03
- Stackhouse S, Brodholt JP, Price GD. 2007. Electronic spin transitions in iron-bearing MgSiO₃ perovskite. *Earth Planet. Sci. Lett.* 253:282–90
- Sturhahn W, Jackson JM, Lin JF. 2005. The spin state of iron in minerals of Earth's lower mantle. *Geophys. Res. Lett.* 32:L12307
- Tsuchiya T, Wentzcovitch RM, da Silva CRS, de Gironcoli S. 2006. Spin transition in magnesiowüstite in Earth's lower mantle. *Phys. Rev. Lett.* 96:198501**
- Umemoto K, Wentzcovitch RM, Yu YG, Requist R. 2008. Spin transition in (Mg,Fe)SiO₃ perovskite under pressure. *Earth Planet. Sci. Lett.* 276:198–206
- Wentzcovitch RM, Justo JF, Wu Z, da Silva CRS, Yuen DA, Kohlstedt D. 2009. Anomalous compressibility of ferropericlaase throughout the iron spin cross-over. *Proc. Natl. Acad. Sci. USA* 106:8447–52



Contents

Falling in Love with Waves <i>Hiroo Kanamori</i>	1
The Diversity of Large Earthquakes and Its Implications for Hazard Mitigation <i>Hiroo Kanamori</i>	7
Broadband Ocean-Bottom Seismology <i>Daisuke Suetsugu and Hajime Shiobara</i>	27
Extrasolar Cosmochemistry <i>M. Jura and E.D. Young</i>	45
Orbital Climate Cycles in the Fossil Record: From Semidiurnal to Million-Year Biotic Responses <i>Francisco J. Rodríguez-Tovar</i>	69
Heterogeneity and Anisotropy of Earth's Inner Core <i>Arwen Deuss</i>	103
Detrital Zircon U-Pb Geochronology Applied to Tectonics <i>George Gebrels</i>	127
How Did Early Earth Become Our Modern World? <i>Richard W. Carlson, Edward Garnero, T. Mark Harrison, Jie Li, Michael Manga, William F. McDonough, Sujoy Mukhopadhyay, Barbara Romanowicz, David Rubie, Quentin Williams, and Shijie Zhong</i>	151
The Stardust Mission: Analyzing Samples from the Edge of the Solar System <i>Don Brownlee</i>	179
Paleobiology of Herbivorous Dinosaurs <i>Paul M. Barrett</i>	207
Spin Transitions in Mantle Minerals <i>James Badro</i>	231
Mercury Isotopes in Earth and Environmental Sciences <i>Joel D. Blum, Laura S. Sherman, and Marcus W. Johnson</i>	249

Investigating Microbe–Mineral Interactions: Recent Advances in X-Ray and Electron Microscopy and Redox–Sensitive Methods <i>Jennyfer Miot, Karim Benzerara, and Andreas Kappler</i>	271
Mineralogy of the Martian Surface <i>Bethany L. Ehlmann and Christopher S. Edwards</i>	291
The Uses of Dynamic Earthquake Triggering <i>Emily E. Brodsky and Nicholas J. van der Elst</i>	317
Short-Lived Climate Pollution <i>R.T. Pierrehumbert</i>	341
Himalayan Metamorphism and Its Tectonic Implications <i>Matthew J. Kohn</i>	381
Phenotypic Evolution in Fossil Species: Pattern and Process <i>Gene Hunt and Daniel L. Rabosky</i>	421
Earth Abides Arsenic Biotransformations <i>Yong-Guan Zhu, Masafumi Yoshinaga, Fang-Jie Zhao, and Barry P. Rosen</i>	443
Hydrogeomorphic Effects of Explosive Volcanic Eruptions on Drainage Basins <i>Thomas C. Pierson and Jon J. Major</i>	469
Seafloor Geodesy <i>Roland Bürgmann and David Chadwell</i>	509
Particle Geophysics <i>Hiroyuki K.M. Tanaka</i>	535
Impact Origin of the Moon? <i>Erik Asphaug</i>	551
Evolution of Neogene Mammals in Eurasia: Environmental Forcing and Biotic Interactions <i>Mikael Fortelius, Jussi T. Eronen, Ferhat Kaya, Hui Tang, Pasquale Raia, and Kai Puolamäki</i>	579
Planetary Reorientation <i>Isamu Matsuyama, Francis Nimmo, and Jerry X. Mitrovica</i>	605
Thermal Maturation of Gas Shale Systems <i>Sylvain Bernard and Brian Horsfield</i>	635
Global Positioning System (GPS) and GPS–Acoustic Observations: Insight into Slip Along the Subduction Zones Around Japan <i>Takuya Nishimura, Mariko Sato, and Takeshi Sagiya</i>	653
On Dinosaur Growth <i>Gregory M. Erickson</i>	675

Diamond Formation: A Stable Isotope Perspective <i>Pierre Cartigny, Médéric Palot, Emilie Thomassot, and Jeff W. Harris</i>	699
Organosulfur Compounds: Molecular and Isotopic Evolution from Biota to Oil and Gas <i>Alon Amrani</i>	733

Indexes

Cumulative Index of Contributing Authors, Volumes 33–42	769
Cumulative Index of Article Titles, Volumes 33–42	774

Errata

An online log of corrections to *Annual Review of Earth and Planetary Sciences* articles may be found at <http://www.annualreviews.org/errata/earth>



ANNUAL REVIEWS

It's about time. Your time. It's time well spent.

New From Annual Reviews:

Annual Review of Statistics and Its Application

Volume 1 • Online January 2014 • <http://statistics.annualreviews.org>

Editor: **Stephen E. Fienberg**, *Carnegie Mellon University*

Associate Editors: **Nancy Reid**, *University of Toronto*

Stephen M. Stigler, *University of Chicago*

The *Annual Review of Statistics and Its Application* aims to inform statisticians and quantitative methodologists, as well as all scientists and users of statistics about major methodological advances and the computational tools that allow for their implementation. It will include developments in the field of statistics, including theoretical statistical underpinnings of new methodology, as well as developments in specific application domains such as biostatistics and bioinformatics, economics, machine learning, psychology, sociology, and aspects of the physical sciences.

Complimentary online access to the first volume will be available until January 2015.

TABLE OF CONTENTS:

- *What Is Statistics?* Stephen E. Fienberg
- *A Systematic Statistical Approach to Evaluating Evidence from Observational Studies*, David Madigan, Paul E. Stang, Jesse A. Berlin, Martijn Schuemie, J. Marc Overhage, Marc A. Suchard, Bill Dumouchel, Abraham G. Hartzema, Patrick B. Ryan
- *The Role of Statistics in the Discovery of a Higgs Boson*, David A. van Dyk
- *Brain Imaging Analysis*, F. DuBois Bowman
- *Statistics and Climate*, Peter Guttorp
- *Climate Simulators and Climate Projections*, Jonathan Rougier, Michael Goldstein
- *Probabilistic Forecasting*, Tilmann Gneiting, Matthias Katzfuss
- *Bayesian Computational Tools*, Christian P. Robert
- *Bayesian Computation Via Markov Chain Monte Carlo*, Radu V. Craiu, Jeffrey S. Rosenthal
- *Build, Compute, Critique, Repeat: Data Analysis with Latent Variable Models*, David M. Blei
- *Structured Regularizers for High-Dimensional Problems: Statistical and Computational Issues*, Martin J. Wainwright
- *High-Dimensional Statistics with a View Toward Applications in Biology*, Peter Bühlmann, Markus Kalisch, Lukas Meier
- *Next-Generation Statistical Genetics: Modeling, Penalization, and Optimization in High-Dimensional Data*, Kenneth Lange, Jeanette C. Papp, Janet S. Sinsheimer, Eric M. Sobel
- *Breaking Bad: Two Decades of Life-Course Data Analysis in Criminology, Developmental Psychology, and Beyond*, Elena A. Erosheva, Ross L. Matsueda, Donatello Telesca
- *Event History Analysis*, Niels Keiding
- *Statistical Evaluation of Forensic DNA Profile Evidence*, Christopher D. Steele, David J. Balding
- *Using League Table Rankings in Public Policy Formation: Statistical Issues*, Harvey Goldstein
- *Statistical Ecology*, Ruth King
- *Estimating the Number of Species in Microbial Diversity Studies*, John Bunge, Amy Willis, Fiona Walsh
- *Dynamic Treatment Regimes*, Bibhas Chakraborty, Susan A. Murphy
- *Statistics and Related Topics in Single-Molecule Biophysics*, Hong Qian, S.C. Kou
- *Statistics and Quantitative Risk Management for Banking and Insurance*, Paul Embrechts, Marius Hofert

Access this and all other Annual Reviews journals via your institution at www.annualreviews.org.

ANNUAL REVIEWS | Connect With Our Experts

Tel: 800.523.8635 (US/CAN) | Tel: 650.493.4400 | Fax: 650.424.0910 | Email: service@annualreviews.org

